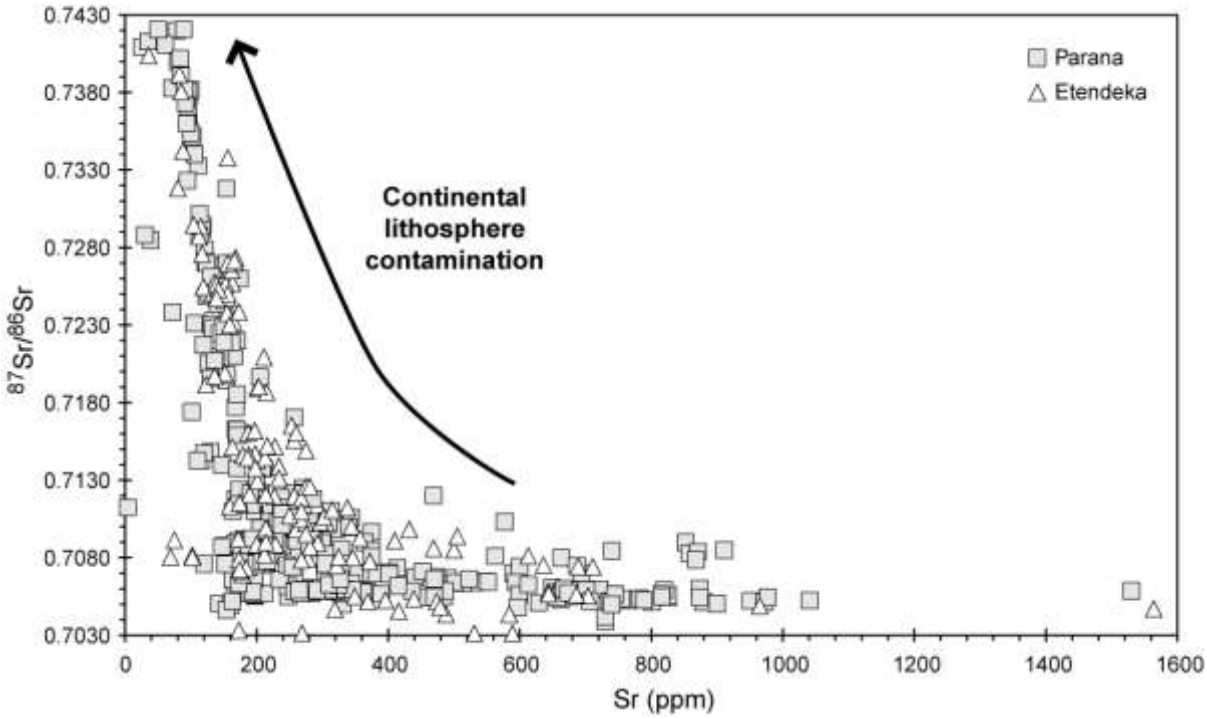

Supplementary Figure 1: Sr concentration versus $^{87}Sr/^{86}Sr$ isotope ratio for Parana and Etendeka flood basalts, showing that melts with low Sr concentrations are the most susceptible to continental lithosphere contamination.

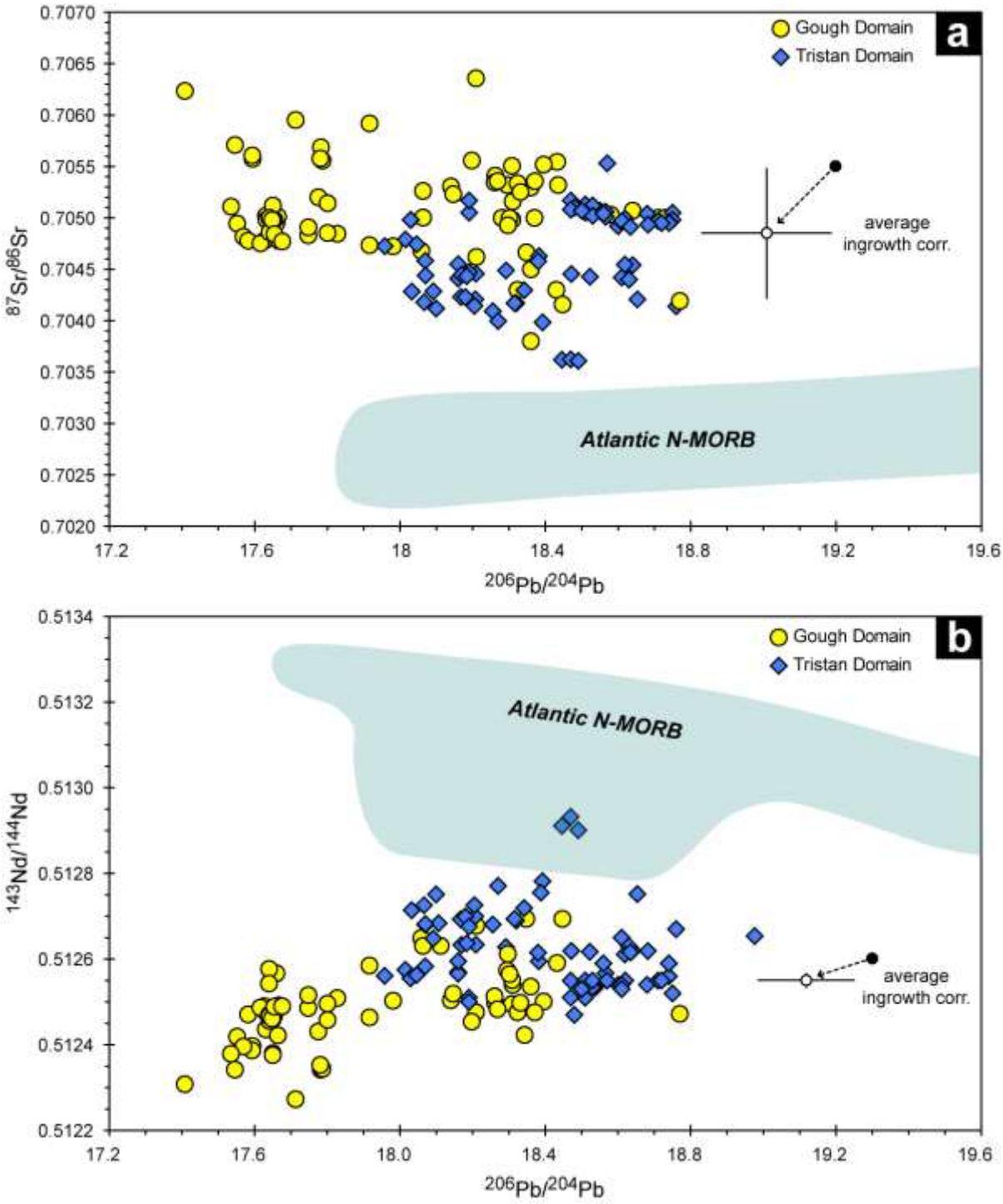

Supplementary Figure 2: Isotope correlation diagrams for **(a)** $^{206}Pb/^{204}Pb$ versus $^{87}Sr/^{86}Sr$ and **(b)** $^{206}Pb/^{204}Pb$ versus $^{143}Nd/^{144}Nd$ showing that the Tristan domain is generally shifted towards N-MORB relative to the Gough domain. Average radiogenic ingrowth correction and 1σ variation as defined in the figure 2 caption.

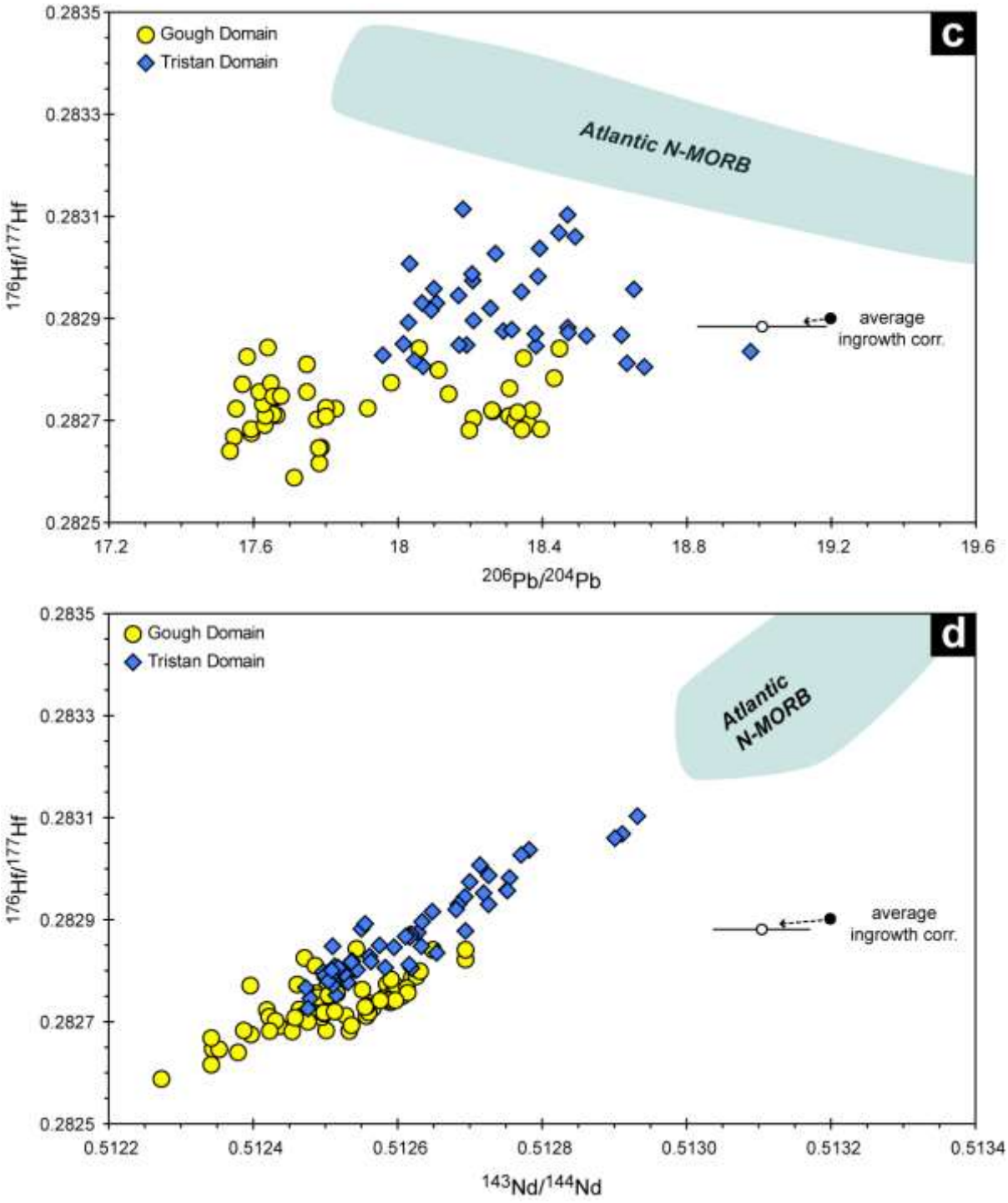

Supplementary Figure 2 continued: Isotope correlation diagrams for **(c)** $^{206}Pb/^{204}Pb$ versus $^{176}Hf/^{177}Hf$ and **(d)** $^{143}Nd/^{144}Nd$ versus $^{176}Hf/^{177}Hf$, showing that the Tristan domain is generally shifted towards N-MORB relative to the Gough domain. Average radiogenic ingrowth correction and 1σ variation as defined in the figure 2 caption.

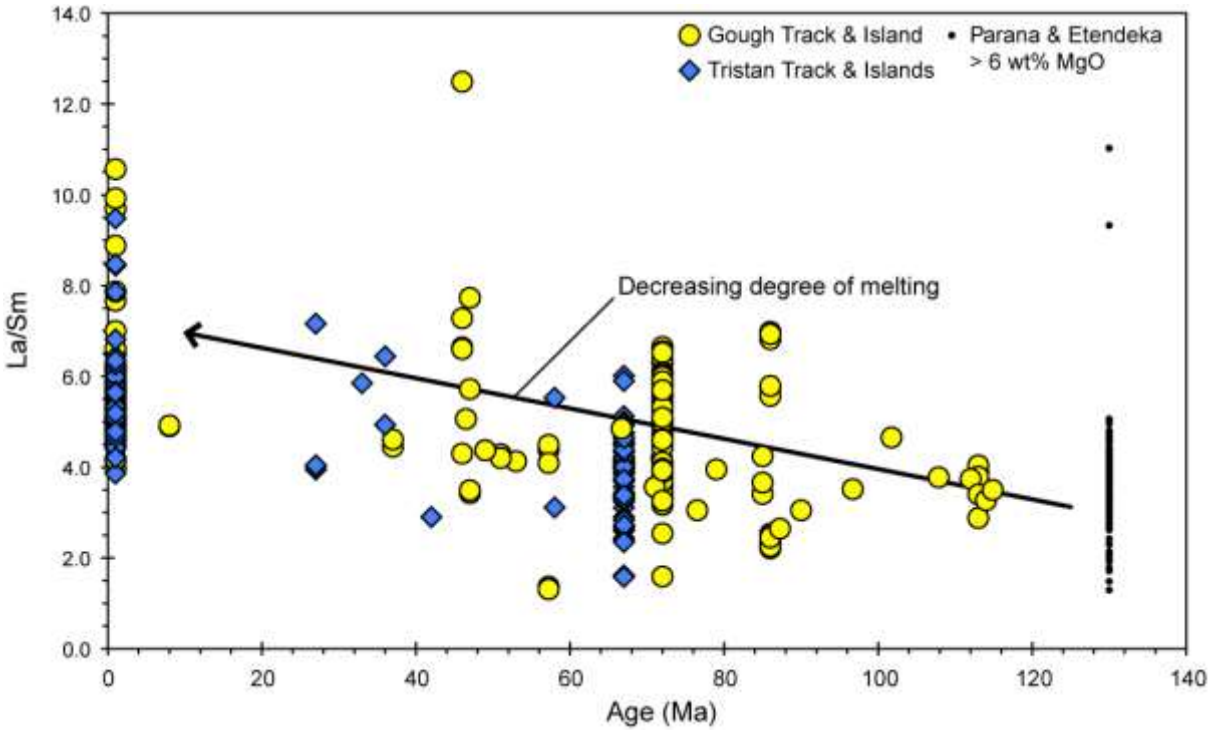

Supplementary Figure 3: Age versus La/Sm diagram for the Tristan-Gough hotspot track evolution.